Reprinted from Applied Optics, Vol. 25, Page 1170, April 1, 1986

Calibration of a sunphotometer by simultaneous measurements of direct-solar and circumsolar radiations

Masayuki Tanaka, Teruyuki Nakajima, and Masataka Shiobara

A new method is proposed for the calibration of the sunphotometer. Well-known difficulties of the usual Langley-plot method when applied to unsteady turbidity conditions can be avoided by monitoring the circumsolar radiation. To realize this idea, an alternate of the Langley-plot method is developed, in which the logarithm of the sunphotometer reading is plotted against the ratio of intensity of singly scattered circumsolar radiation to that of direct solar radiation instead of the optical air mass in the usual Langley-plot method. Results of numerical simulations and field tests with a newly developed instrument show that the rms error of the calibration constant could be reduced to 1/5–1/10 of the usual method for wavelengths larger than 500 nm.

I. Introduction

Concerns about the role of aerosol optical properties in the atmosphere and their effects on local and global climate have led to widespread use of sunphotometers.[1–6] The maintenance of the calibration constants of sunphotometers is essential in such works, especially for monitoring of long-term variations of atmospheric turbidity. The possibility of errors in the calibrations and observed discrepancy of results among instruments[7–9] have led the specialists to perform an extensive intercomparison of several sunphotometers of different designs, but resulting large uncertainties in calibration constants suggested the difficulty inherent in the usual Langley-plot method.[10] The Langley-plot method assumes that the atmosphere is temporarily invariant and horizontally homogeneous during the measurements at different solar zenith angles. Especially, the assumption of temporal stability of the atmosphere can hardly be satisfied at least at usual locations. Shaw[11,12] pointed out that almost all calibrations of sunphotometers conducted at continental locations have the possibility of being seriously marred because of time changing drifts in atmospheric turbidity. He also pointed out the fact that time variations in atmospheric turbidity often have systematic trends of a type that provides a nearly linear Langley plot.

Recently, some possibility of diagnostic use of the solar aureole data in the calibration of sunphotometers has been suggested by O'Neill and Miller[13] and by ourselves.[14] Since the aureole intensity is approximately proportional to the optical thickness of the atmosphere, the time variation of atmospheric turbidity during the calibration can be known from simultaneous measurements of the aureole intensity. In Sec. II we show how the circumsolar radiation can be incorporated into the calibration of sunphotometers adopting the ratio of the intensity of circumsolar radiation to that of direct solar radiation as a new variable instead of the optical air mass in the usual Langley-plot method. Results of numerical simulation and field tests are presented in Secs. III and IV, respectively.

II. Theoretical Basis

The Langley-plot method is based on Beer's law:

$$\ln F = \ln F_0 - m\tau, \tag{1}$$

where F and F_0 are intensities of solar radiation received at the bottom and top of the atmosphere, respectively, m is the optical air mass, and τ is the normal optical thickness of the atmosphere. The extrapolation of the plot of $\ln F$ vs m to the $m = 0$ point allows us to know the radiometer reading at the top of the atmosphere, i.e., the calibration constant, if the atmosphere is horizontally homogeneous and the optical thickness does not change during the calibration. However, linearity of the Langley plot does not always assure the successful extrapolation. As pointed out by Shaw,[11,12] we get an incorrect value $F_0 \exp(-\tau_2)$ instead of F_0

When this work was done all authors were with Tohoku University, Faculty of Science, Upper Atmosphere Research Laboratory, Sendai 980, Japan; M. Shiobara is now with Meteorological Research Institute, Tsukuba, Ibaraki 305, Japan.

Received 30 July 1985.
0003-6935/86/071170-07$02.00/0.

when the optical thickness varies with m as $\tau = \tau_1 + \tau_2/m$ or parabolically with time from noon as $\tau(t) = \tau_1' + \tau_2' t^2$. Thus we become aware of the necessity of monitoring the variation of atmospheric turbidity during the calibration.

The idea of using the circumsolar radiation for monitoring atmospheric turbidity can be traced back to the solar constant program of the Smithsonian Astrophysical Observatory.[15,16] They utilized empirically the data of circumsolar radiation (i.e., pyranometer readings) to correct the attenuation of direct solar radiation due to aerosols in their short method. Deirmendjian[17] suggested the availability of the circumsolar radiation for quantitative detection of very small amounts of aerosols and other particulates and of small changes in their concentration, size, and composition. He proposed an aureole theory in the form of a first-order perturbation of the well-known Rayleigh scattering field. O'Neill and Miller[13] and ourselves[14] suggested more directly the use of the circumsolar radiation in the calibration of sunphotometers.

The single-scattering approximation of the aureole intensity in the almucantar of the sun is given by

$$F_a^1(\mu_0,\phi) = m\tau\omega_0 P(\cos\Theta) F_0 \exp(-m\tau)\Delta\Omega, \quad (2)$$

where μ_0 is the cosine of the solar zenith angle, ϕ is the azimuthal angle measured from the solar principal plane, ω_0 is the single scattering albedo, $P(\cos\Theta)$ is the normalized phase function at the scattering angle Θ, $\Delta\Omega$ is the solid viewing angle of the radiometer, and $\cos\Theta = \mu_0^2 + (1 - \mu_0^2)\cos\phi$. Thus the intensity of singly scattered radiation in the solar almucantar is proportional to the optical thickness. The quantities τ, ω_0, and $P(\cos\Theta)$ in Eq. (2) are sums of respective contributions of aerosols and air molecules given by

$$\tau = \tau_a + \tau_m, \quad (3)$$

$$\omega_0 = (\omega_{0a}\tau_a + \omega_{0m}\tau_m)/\tau, \quad (4)$$

$$P(\cos\Theta) = [\omega_{0a}\tau_a P_a(\cos\Theta) + \omega_{0m}\tau_m P_m(\cos\Theta)]/\omega_0\tau, \quad (5)$$

where τ_a, ω_{0a}, and $P_a(\cos\Theta)$ are the optical thickness, the single-scattering albedo, and the phase function of aerosols, respectively; and τ_m, ω_{0m}, and $P_m(\cos\Theta)$ are corresponding quantities of air molecules. The phase function is defined to satisfy the normalization integral of

$$2\pi \int_{-1}^{1} P(x)dx = 1.$$

If we measure the intensity of direct solar radiation and that of circumsolar radiation from a given portion of the aureole region simultaneously by a single radiometer, the relation in Eq. (1), when combined with Eq. (2), can be written as

$$\ln F = \ln F_0 - \tau^*, \quad (6)$$

$$\tau^* = m\tau = F_a^1/[F\Delta\Omega\omega_0 P(\cos\Theta)]. \quad (7)$$

The above equations show that the value of F_0 can be obtained by extrapolating the plot of $\ln F$ vs optical thickness of the slant path τ^* (or equivalently the ratio F_a^1/F) to the point of $\tau^* = 0$ (or $F_a^1/F = 0$), if the factors in the Eq. (7) other than the diffuse-to-direct ratio F_a^1/F do not change during the calibration. Figure 1 shows the normalized phase functions of aerosols $P_a(\cos\Theta)$ for different size distribution functions. The magnitudes of $P_a(\cos\Theta)$ are more or less independent of the size distribution of aerosols at scattering angles around 20°. Although the single-scattering albedo of aerosols ω_{0a} depends on aerosol models, it remains unchanged if the size distribution and chemical composition of aerosols do not change during the calibration.

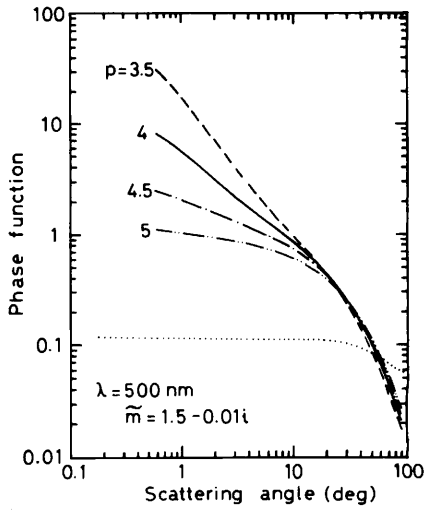

Fig. 1. Normalized phase functions of aerosols ($p = 3.5 \sim 5$) and air molecules (dotted line). The parameter p is the exponent of the size distribution function of aerosols in Eq. (10). The index of refraction of aerosols is assumed to be $\tilde{m} = 1.5\text{–}0.01i$.

Thus, if the effect of molecular scattering is negligible or corrected precisely, the extrapolation by Eq. (6) is promising for the evaluation of calibration constant F_0 under turbidity conditions actually occurring. The quantity which can be estimated from the ratio F_a^1/F is not τ but $\omega_0\tau$ unless the complex index of refraction of aerosols is given *a priori*.[18] The use of the diffuse-to-direct ratio F_a^1/F is essential to compensate the extrapolation error due to the temporal change of the optical thickness during the calibration. It is expected that the extrapolated value of F_0 depends more or less on the change of optical properties of aerosols occurring in parallel with the change of atmospheric turbidity. This expectation will be examined by numerical simulations in the next section.

Unfortunately, the above simple idea does not apply to real conditions of the atmosphere since the contribution of multiple scattering cannot be neglected, and the normalized phase function in Eq. (7) is affected seriously by the ratio of the optical thickness of aerosols to that of air molecules.[17] The normalized phase function $P_m(\cos\Theta)$ of air molecules crosses those of aerosols at scattering angles around 60°. However, we are reluctant to adopt such a large scattering angle for the turbidity monitoring because of the high dependency of the normalized phase function of aerosols on their size distribution as well as a large contribution of

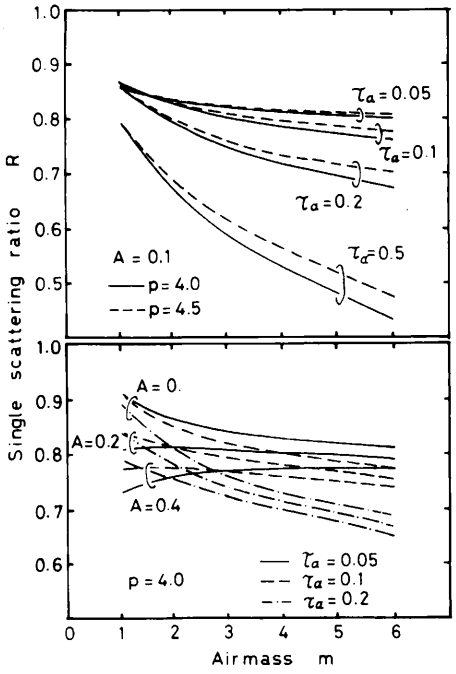

Fig. 2. Single-scattering ratio R as a function of the optical air mass m for $\lambda = 500$ nm, $\tau_m = 0.139$, $\Theta = 20°$, $\tilde{m} = 1.5\text{–}0.01i$, and various values of τ_a, p, and A. The upper panel shows the dependence of R on τ_a and p at $A = 0.1$ and the lower panel the dependence of R on τ_a and A at $p = 4.0$.

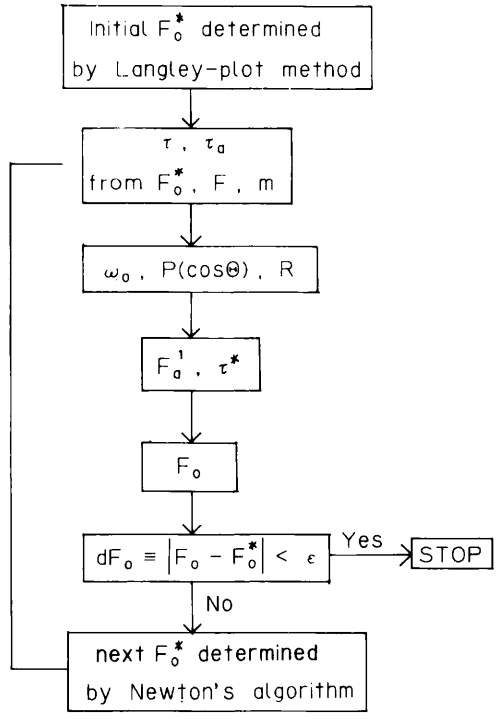

Fig. 3. Iteration scheme to determine the calibration constant from measurements of direct-solar and circumsolar radiations.

multiple scattering to measured diffuse radiation. Adopting the scattering angle of 20°, we calculate the normalized phase function of the atmosphere by Eq. (5) and estimate the intensity of singly scattered radiation F_a^1 from the measured intensity F_a by

$$F_a^1 = R(m,\tau_a,\tau_m,\tilde{m},A,\Theta)F_a, \tag{8}$$

where the quantity R is the ratio of the intensity of singly scattered radiation to that of total radiation, referred to as the single-scattering ratio.

The value of R depends on several parameters, such as the optical air mass m, optical thicknesses of aerosols and air molecules, τ_a and τ_m, complex index of refraction of aerosols $\tilde{m}$, ground albedo A, and scattering angle Θ. It is expected, however, that the extrapolation of Eq. (6) depends rather weakly on these parameters. We can, therefore, prepare a library of proper size for R assuming typical aerosol models and ground albedos. Figure 2 illustrates the values of R against the optical air mass m for $\lambda = 500$ nm and various values of τ_a, p, and A. The contribution of multiple scattering to the total diffuse radiation exceeds 10% even for optical thicknesses of aerosols as small as 0.05.

To estimate the intensity of singly scattered radiation from measured aureole intensity and to obtain the extrapolated value F_0, we adopt an iteration scheme as shown in Fig. 3. The measured quantities are the intensities of direct-solar and circumsolar radiations, F and F_a, and the optical air mass m. As for the size distribution and complex index of refraction of aerosols and ground albedo, we have to adopt a specific model typical for that location and season. The single-scattering albedo ω_{0a}, normalized phase function $P_a(\cos\Theta)$, and optical thickness τ_a of aerosols are estimated theoretically for that aerosol model. Figure 3 shows the ith step of the iteration. The calibration constant just before the ith step is denoted by F_0^*. Using this value of F_0^* and measured values of F and m, optical thickness $\tau_{(i)}$ and $\tau_{a(i)}$ are obtained from Eqs. (1) and (2). The single-scattering albedo $\omega_{0(i)}$ of the turbid atmosphere is estimated from these values of $\tau_{(i)}$ and $\tau_{a(i)}$ by Eq. (4). The normalized phase function $P_{(i)}(\cos\Theta)$ is also obtained from $\tau_{(i)}$, $\tau_{a(i)}$, and $\omega_{0(i)}$ by Eq. (5). The single-scattering ratio $R_{(i)}$ can be estimated by applying the radiative transfer code of Nakajima *et al.*[18] to the model atmosphere thus obtained. The quantities F_a^1 and τ^* are now given straightforwardly from Eqs. (8) and (7), respectively, and consequently the calibration constant $F_{0(i)}$ from the least-square regression of Eq. (6). The iteration is terminated when the convergence criterion

$$|F_{0(i)} - F_0^*| \equiv |dF_{0(i)}| < \epsilon \tag{9}$$

is satisfied. If it is not the case, steps are repeated by replacing F_0^* with the solution of the equation $dF_0 = 0$, which is obtained from the values of $dF_{0(i-1)}$ and $dF_{0(i)}$ by Newton's algorithm. Obviously, the uncertainty in the viewing angle $\Delta\Omega$ does not affect the result of calibration. Uncertainties in ω_0 and $P(\cos\Theta)$ do not also affect the calibration constant if they are unchangeable during the calibration.

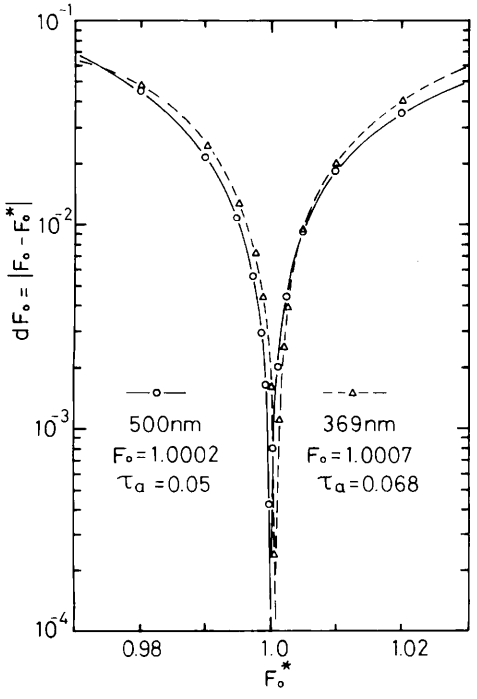

Fig. 4. Absolute values of dF_0 ($=|F_0 - F_0^*|$) vs F_0^*. The solid line corresponds to λ = 500 nm and τ_a = 0.05 and the dashed line to λ = 369 nm and τ_a = 0.068.

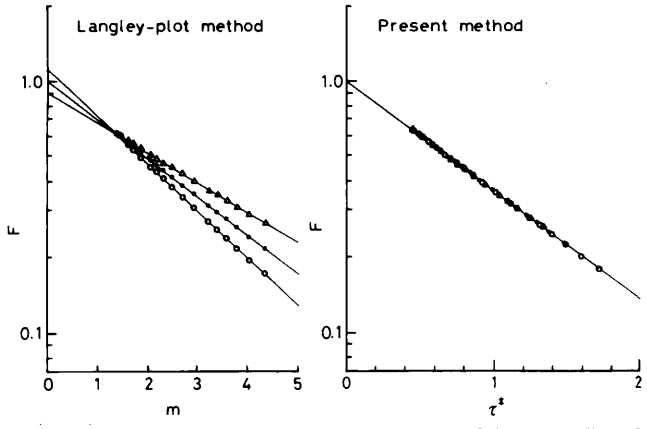

Fig. 5. Comparisons of the Langley-plot method (left panel) and the present method (right panel) at λ = 500 nm for turbidity conditions given in Eq. (9) with the optical thickness of aerosols at noon τ_{a0} = 0.2 and Shaw's parabolic drift parameter α = 0, ●; 0.011, △; and −0.011, ○.

III. Numerical Simulations

Numerical simulations were carried out to examine the ability of the calibration method mentioned in the previous section. Theoretical values were substituted for the intensities of direct-solar and circumsolar radiations, assuming the size distribution and complex index of refraction of aerosols as

$$n(r) = \begin{cases} C \cdot 10^{p} & \text{for } r < 0.1\ \mu\text{m}, \\ C \cdot r^{-p} & \text{for } r > 0.1\ \mu\text{m}, \end{cases} \tag{10}$$

and $\tilde{m}$ = 1.50–0.01i, respectively, where $n(r)dr$ is the number density of particles between radii r and $r + dr$. The most typical value of the exponent p is 4.2 in continental air masses prevailing in the cold season in Sendai, Japan.[19]

Figure 4 shows the values of the function dF_0 against F_0^* for λ = 369 nm (broken line) and 500 nm (solid line). True values of the calibration constants are assumed to be unity for both cases. Very acute minima of dF_0 are found at F_0 = 1.0002 and 1.0007 for 369 and 500 nm, respectively, i.e., just around the true values. It can be expected from the figure that uncertainties in the calibration constant are less than ±0.5% if the rms error of the data does not exceed the limit of ±1%.

The parabolic variation of the optical thickness with time gives a straight Langley plot as suggested by Shaw.[11] In Fig. 5 and Table I are shown the results of numerical simulation for turbidity conditions varying as

$$\tau_a(t) = \tau_{a0}(1 + \alpha t^2), \tag{11}$$

where τ_{a0} is the optical thickness of aerosols at noon, α is Shaw's parabolic drift parameter, and t is the time difference (in hours) from noon. The values of α were assumed to be 0, 0.011, and −0.011; corresponding changes of τ_a are 0, 10, and −10% for 3 h around noon. Simulated data were adopted for seventeen values of the optical air mass ranging from 4.5 to 1.5. It is evident that the usual Langley-plot method predicts systematically larger or smaller values of F_0 for finite values of α in spite of an excellent linearity in the respective plots, while the prediction by Eq. (6) is independent of the values of α. The uncertainty in F_0 is less than ±0.3% for our method, whereas that for the

Table I. Comparison of Simulated Calibration Between the Present and Langley-plot Methods for Turbidity Conditions Varying Parabolically with Time*

wavelength		369nm			500nm			862nm		
τ_{a0}		0.072	0.144	0.288	0.05	0.1	0.2	0.026	0.052	0.104
α = 0.0	Present	0.9993	0.9994	0.9994	0.9995	1.0002	1.0004	1.0001	1.0000	0.9997
	Langley	0.9995	0.9995	0.9993	0.9998	0.9998	0.9997	1.0000	0.9999	0.9999
α = 0.011	Present	0.9995	0.9994	0.9970	0.9998	1.0001	0.9988	0.9999	0.9998	0.9994
	Langley	1.0375	1.0768	1.1600	1.0260	1.0529	1.1087	1.0135	1.0272	1.0552
α = −0.011	Present	1.0009	0.9998	1.0015	0.9997	0.9996	0.9997	1.0001	1.0000	0.9999
	Langley	0.9630	0.9277	0.8609	0.9743	0.9493	0.9014	0.9866	0.9734	0.9475

* τ_{a0} is the optical thickness of aerosols at noon and α is Shaw's parabolic drift parameter. True values of the calibration constants are assumed to be unity.

Table II. Comparison of Simulated Calibration Between the Present and Langley-plot Methods for Size Distributions Differing from Assumed One*

wavelength		369nm		500nm		862nm	
$\tau_{a,500}$		0.05	0.1	0.05	0.1	0.05	0.1
p=4.0	Present	0.9973	0.9938	0.9987	0.9971	0.9997	0.9990
	Langley	0.9996	0.9996	0.9998	0.9998	1.0000	1.0000
p=4.5	Present	1.0032	1.0075	1.0016	1.0031	1.0004	1.0009
	Langley	0.9996	0.9995	0.9998	0.9998	1.0000	1.0000
p=4.0→4.5	Present	0.9984	0.9956	0.9984	0.9947	0.9984	0.9965
	Langley	0.9837	0.9681	0.9999	0.9998	1.0114	1.0229
p=4.5→4.0	Present	1.0066	1.0152	1.0062	1.0134	1.0051	1.0109
	Langley	1.0239	1.0486	0.9998	0.9998	0.9860	0.9722

* $\tau_{a,500}$ is the optical thickness of aerosols at λ=500nm and p is the exponent of the size distribution function given in Eq.(10). The value of p is assumed to be 4.2 in the simulation.

usual Langley-plot method amounts to ±15% for α = ±0.011 (Table I).

Since the single-scattering ratio R depends on many optical parameters of the atmosphere, it is necessary to examine the effect of these parameters on the result of extrapolation by Eq. (6). Table II shows the error in F_0 when the assumed size distribution of aerosols differs from the true distribution. In the first two cases, the value of the exponent p in Eq. (10) was assumed to be 4.2 instead of its true values of 4.0 and 4.5, respectively. Obviously, the Langley-plot method is free from such kind of error. The error of our method increases with an increase (or a decrease) of the optical thickness of aerosols (or wavelength). The maximum error amounts to 0.75% for p = 4.5 and λ = 369 nm. The succeeding two cases show the error when the size distribution of aerosols changes during the observation. A fixed value of 4.2 was assumed for the exponent p instead of its true values changing from 4.0 to 4.5 and from 4.5 to 4.0, with optical air masses changing from 4.5 to 1.5. Since we assumed fixed values of 0.05 and 0.1 for the optical thickness of aerosols at λ = 500 nm, optical thicknesses are changeable with the temporal variation of the exponent p for the other wavelengths. By this effect, results of the Langley-plot method are also affected by the change of the size distribution of aerosols. The maximum error of our method is ~1.5%, whereas that of the Langley-plot method amounts to 5%.

Table III shows the error when the assumed value of the complex index of refraction of aerosols differs from the true value. The Langley-plot method is independent of such kind of error. The result of our method is more influenced by the error in the imaginary part than that in the real part of the index of refraction of aerosols. This tendency is attributed to the fact that the diffuse intensity decreases with a decrease of the optical air mass more rapidly for smaller values of the imaginary part and vice versa. The value of F_0 is, therefore, overestimated or underestimated according to the overestimation or underestimation of the value of the imaginary part. The errors of our method are within ±1%, except for the case of λ = 369 nm, τ_a = 0.288, and m_i = 0.03, for which the error amounts to 4%.

In addition, to examine the effect of short-time variations of atmospheric turbidity or of observation error, we applied our calibration scheme to the simulated data with random errors of σ = 0.5% but showing no diurnal trend of τ_a. Our scheme is found to be fairly independent of such random errors as in the usual Langley-plot method. The rms errors of the calibration constant obtained from twenty independent runs are 0.25 and 0.41% at λ = 500 nm and 0.25 and 0.29% at λ = 862 nm for the present method and the Langley-plot method, respectively.

IV. Verification of the Method by Observations

The validity of the method was examined by applying for the actual data obtained in Sendai, Japan. The instrument used was a scanning radiometer (aureolemeter) which can measure both direct-solar and circumsolar radiations almost simultaneously. A silicon photodiode (Hamamatsu Photonics Co., S1336-8BQ) and interference filters with central wavelengths of 369, 500, 675, 776, and 862 nm (Koshin Kogaku Co., BWB series) were used as the detector and monochromator, respectively. The full field-of-view angle of the radiometer is ~1.0°, which alows us to aim at the solar disk without difficulty. A well-designed sun-shade hood of 65-cm length allows the measurement of the aureole intensity at scattering angles of Θ = 1.5° without serious contamination of the reflected solar radiation. The aureolemeter is mounted on an equatorial driven by a clock-synchronous motor, which is further mounted on a horizontal turntable. Further informations of the aureolemeter are shown in Table IV.

The results of calibration by the present method are shown in Fig. 6 and in more detail in Table V. The complex index of refraction of aerosols and the ground albedo are assumed to be 1.50–0.01i and 0.1, respectively. In Fig. 6, we plotted ln$F$ against $\tau^*\Delta\Omega$ instead of τ^* or F_a^1/F, because the calibration of the viewing angle of the radiometer was not established. It is expected from Eqs. (6) and (7) that all data points are

Table III. Results of Simulated Calibration for the Complex Index of Refraction Differing from the Assumed Value of 1.5–0.01i

wavelength	369nm			500nm			862nm		
τ_a	0.072	0.144	0.288	0.05	0.1	0.2	0.026	0.052	0.104
$\tilde{m}$ = 1.50-0.0i	0.9980	0.9905	0.9703	0.9983	0.9973	0.9911	0.9996	0.9989	0.9969
1.50-0.03i	1.0036	1.0094	1.0404	1.0019	1.0037	1.0115	1.0003	1.0013	1.0034
1.45-0.01i	0.9983	0.9977	0.9944	1.0000	0.9979	0.9920	0.9994	0.9990	0.9970
1.55-0.01i	1.0013	1.0016	1.0013	1.0008	1.0018	1.0052	1.0002	1.0006	1.0017

Table IV. Specifications of the Aureolemeter

Interference filters: Koshin Kogaku Co., BWB series with wavelengths (bandwidths) of 369(7), 500(4), 675(6), 776(7), 862(8) (nm) blocking in both wings: < 0.01% in transmittance for all filters
Detector: Hamamatsu Photonics Co., Silicon photodiode, S1336-8BQ
Object lens: Canon, FD200 (50mm diam.)
Sun-shade hood: 65 cm
Full field-of-view angle: 1.0°
Minimum observable angle: 1.25°
Precision of the azimuthal-angle controller: 0.25°
Electrical dynamic range: 10^5
Driving: Equatorial mounted on a horizontal turntable

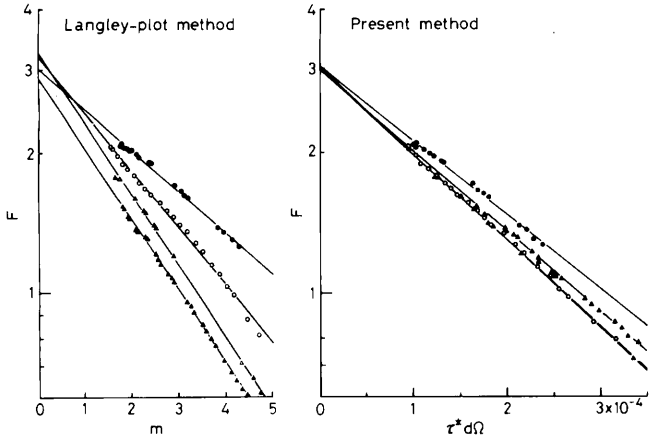

Fig. 6. Comparisons of the Langley-plot method (left panel) and the present method (right panel) at λ = 500 nm for measured data of 15 Oct. 1981, ○; 10 Nov. 1981, ●; 16 Feb. 1982, △; and 18 Feb. 1982, ▲.

plotted on a single regression line of slope $\Delta\Omega$, if optical properties of aerosols are exactly known. Separation of the respective plots into respective regression lines is, therefore, attributed to uncertainties in aerosol models. Nevertheless, uncertainty of the calibration constant is much smaller for the present method than for the Langley-plot method. In Table V, we first analyzed the data by assuming the value of the exponent p to be 4.2 (Method F) and then reanalyzed the data by use of the exponent estimated from the log–log plot of the optical thickness of aerosols vs wavelength (Method P). The difference between both treatments is insignificant, as expected from the result of simulation shown in Table II. The rms errors of our method are ~3% for λ = 369 nm and 0.5% for the other wavelengths, while those of the Langley-plot method (Method L) are ~3% for all wavelengths. The rms errors of the calibration constants are approximately in accord with the rms errors of the respective plots for the present method but are much larger than those of the respective plots for the Langley-plot method. This fact suggests that the results of the Langley-plot method are affected by systematic variations of the optical thickness of aerosols as in Eq. (9). The calibration constants by the Langley-plot method are larger or smaller than those by the present method according to circumstances. This fact suggests the occurrence of both aerosol loadings parabolically increasing and decreasing with time. The magnitudes of the error indicate that the number of times of calibration required for the present method is much smaller than for the Langley-plot method to attain the same accuracy. Large uncertainties for λ = 369 nm may be attributed to several reasons so that the relative sensitivity of our aureolemeter for λ = 369 nm is ~1/10 for the other wavelengths, that the multiple-scattering correction is too large to retrieve the single-scattering intensity with required accuracy, and that the normalized phase function in Eq. (5) is affected significantly by the change in the optical thickness of aerosols due to the large contribution of Rayleigh scattering.

Table V. Calibration of the Aureolemeter by the Present and Langley-plot Methods*

Wavelength		369nm			500nm			862nm		
Method		F	P	L	F	P	L	F	P	L
15 Oct. 1981	F_0	13.43	13.42	14.33	3.035	3.040	3.197	5.341	5.345	5.488
	σ	1.24	1.19	1.32	0.56	0.57	1.38	0.33	0.33	0.84
10 Nov. 1981	F_0	14.52	14.52	13.95	3.043	3.043	3.008	5.346	5.346	5.357
	σ	3.87	3.87	2.36	1.41	1.41	1.04	0.30	0.30	0.41
16 Feb. 1982	F_0	13.93	13.89	13.83	3.027	3.009	3.264	5.342	5.333	5.540
	σ	4.63	4.40	4.67	0.50	0.48	1.33	0.35	0.34	0.65
18 Feb. 1982	F_0	14.56	14.45	12.97	3.008	2.996	2.896	5.280	5.274	5.207
	σ	2.27	2.25	1.76	0.86	0.84	1.14	0.25	0.25	0.30
Mean	F_0	14.11	14.07	13.77	3.028	3.022	3.091	5.327	5.325	5.398
	σ	3.30	3.18	3.61	0.43	0.66	4.75	0.51	0.56	2.76

* Method F: Present method with fixed p value of 4.2.
Method P: Present method with re-analyzed p value.
Method L: Langley-plot method.
F_0 is the calibration constant and σ is its standard deviation in percent.

V. Summary

We presented and evaluated a new method of calibration of the sunphotometer, in which simultaneous measurements of circumsolar radiation are incorporated. The plot of the logarithm of the measured intensity of direct solar radiation vs diffuse-to-direct ratio is shown to be much more effective for the extrapolation of the radiometer reading to zero air mass than the usual Langley-plot method unless the Rayleigh scattering dominates and the multiple scattering is significant. The accuracy of the present method is 5–10 times as high as the Langley-plot method for wavelengths of $\lambda > 500$ nm.

Since the aureole intensity is approximately proportional to $\omega_0\tau$, we can estimate both values of $\omega_0\tau$ and τ from the combined data of direct-solar and circumsolar radiation. It is promising to determine the single-scattering albedo of the turbid atmosphere and the complex index of refraction of aerosols from these quantities. Thus the use of scanning radiometers which are able to measure both direct and circumsolar radiations simultaneously is recommended not only for their advantages in the calibration point of view discussed in this paper but also for monitoring the atmospheric turbidity itself.

References

1. F. E. Volz, "Photometer snit selenphotoelement zur bestimmung der wellenlaugenabhangegkeit der dunsthulung," Arch. Meteorol. Geophys. Bioklimatol. Ser. B **10,** 100 (1959).
2. E. C. Flowers, R. A. McCormick, and K. R. Kurfis, "Atmospheric Turbidity over the U.S., 1961–1966," J. Appl. Meteorol. **8,** 955 (1969).
3. E. C. Flowers, R. A. McCormick, K. R. Kurfis, and T. H. Bilton, "Atmospheric Turbidity Measurements with the Dual-Wavelength Sunphotometer. Observation and Measurement of Atmospheric Pollution," Special Environ. Rep. 3, World Meteorological Organization, Geneva (1974), pp. 463–480.
4. J. T. Peterson, E. C. Flowers, G. J. Berri, C. L. Reynolds, and J. H. Rudisill, "Atmospheric Turbidity over Central North Carolina," J. Appl. Meteorol. **20,** 229 (1981).
5. G. E. Shaw, "Aerosols at Mauna Loa: Optical Properties," J. Atmos. Sci. **36,** 862 (1979).
6. J. M. Prospero, D. L. Savoie, T. N. Carlson, and R. T. Nees, "Monitoring Sahara Aerosol Transport by Means of Atmospheric Turbidity Measurements," in *Saharan Dust: Mobilization, Transport, Deposition,* SCOPE Rep. 14, C. Morales, Ed. (Wiley, Chichester, England, (1979), pp. 171–186.
7. N. S. Laulainen and B. J. Taylor, "The Precision and Accuracy of Volz Sunphotometry," J. Appl. Meteorol. **13,** 298 (1974).
8. P. B. Russell and G. E. Shaw, "Comments on 'The Precision and Accuracy of Volz Sunphotometry,' " J. Appl. Meteorol. **14,** 1206 (1975).
9. F. E. Volz, "Precision and Accuracy of Sunphotometry—A response," J. Appl. Meteorol. **14,** 1209 (1975).
10. E. Dutton and J. DeLuisi, "Results of a Sunphotometer Intercomparison held at Boulder, 19 October to 16 December 1981," NOAA Tech. Memor. ERL ARL-114 (1982).
11. G. E. Shaw, "Error Analysis of Multi-wavelength Sunphotometry," Pure Appl. Geophys. **114,** 1 (1976).
12. G. E. Shaw, "Sun Photometry," Bull. Am. Meteorol. Soc. **64,** 4 (1983).
13. N. T. O'Neill and J. R. Miller, "Combined Solar Aureole and Solar Beam Extinction Measurements. 1: Calibration Considerations," Appl. Opt. **23,** 3691 (1984).
14. S. Kawaguchi, T. Nakazawa, T. Nakajima, M. Tanaka, and T. Yamanouchi, "Remote Sensing of the Antarctic Atmosphere Using a Sunphotometer," Annual Report of Co-operative Research, 1981. National Institute of Polar Research (1982), p. 101.
15. C. G. Abbot, F. E. Fowle, and L. B. Aldrich, Ann. Astrophys. Obs. Smithsonian Inst. **4** (1922).
16. C. G. Abbot, L. B. Aldrich, and F. E. Fowle, Ann. Astrophys. Obs. Smithsonian Inst. **5** (1923).
17. D. Deirmendjian, "Use of Scattering Techniques in Cloud Microphysics Research: I. The Aureole Method," Rand Report R-590-PR, Oct. 1970, The Rand Corp., Santa Monica, CA.
18. T. Nakajima, M. Tanaka, and T. Yamauchi, "Retrieval of the Optical Properties of Aerosols from Aureole and Extinction Data," Appl. Opt. **22,** 2951 (1983).
19. M. Tanaka, T. Takamura, and T. Nakajima, "Refractive Index and Size Distribution of Aerosols as Estimated from Light Scattering Measurements," J. Clim. Appl. Meteorol. **22,** 1253 (1983).